Adsorption dynamics and angular dependency of contaminants on Ru mirror surfaces

M. Catalfano, A. Kanjilal, A. Al-Ajlony, S. S. Harilal, and A. Hassanein

Citation: Journal of Applied Physics **111**, 016103 (2012); doi: 10.1063/1.3675518
View online: http://dx.doi.org/10.1063/1.3675518
View Table of Contents: http://aip.scitation.org/toc/jap/111/1
Published by the American Institute of Physics

Adsorption dynamics and angular dependency of contaminants on Ru mirror surfaces

M. Catalfano,[a] A. Kanjilal, A. Al-Ajlony, S. S. Harilal, and A. Hassanein
Center for Materials Under Extreme Environment, School of Nuclear Engineering, Purdue University, West Lafayette, Indiana 47907, USA

(Received 26 September 2011; accepted 10 December 2011; published online 6 January 2012)

A real time contamination of the Ru surface and corresponding effect on its work function were studied using extreme ultraviolet photoelectron spectroscopy with a 13.5-nm wavelength of light. The change in work function indicates formation of molecular dipoles, oriented outward from the Ru surface. X-ray photoelectron spectroscopy investigations suggest variation in electromagnetic interaction with the components of the adsorbed foreign species when the emission angle from the target surface was changed from 0° to 50°; H_2O and C-O_n show a strong coupling at lower angles and OH dominates at higher angles, whereas carbon is found in the mid-range peaking at 30°. [doi:10.1063/1.3675518]

In order to continue the steady growth of the semiconductor industry, next generation computer chips are required to have features as small as 20 nm. To meet this goal, next generation photolithography systems are looking to employ extreme ultraviolet (EUV) radiation at a wavelength of 13.5 nm. The mirrors to be used in these systems consist of alternating layers of Mo and Si.[1] Because there are concerns about potential oxidation of the surface Si layer, a thin Ru protective layer has often been used on the top Si layer.[1] A Mo/Si multilayer mirror with a Ru capping layer can reflect up to 70% of the EUV light[2] near normal incidence.[3] Ruthenium films can also reflect 92 eV photons at a grazing angle.[4] Since short wavelengths can be attenuated by most materials[5] and even by background gases,[1] an EUV lithography system requires a vacuum chamber. Now, the issue is how to keep the optics clean, as carbonaceous and/or oxidized Ru surfaces are often formed during EUV exposure and, as a consequence, degrade the overall reflectivity of Mo/Si mirrors. Several cleaning processes[1] have been proposed to circumvent and mitigate this problem. In fact, a large number of groups have been working on understanding the processes involved to mitigate the oxidation and/or carbonization of the top Ru layer (Ref. 6 and references therein).[6] It has so far been established that the secondary electrons from the Ru surface mainly take part in dissociating hydrocarbons and/or water molecules under EUV radiation,[6] creating chemically active fragments on the Ru surface.[7] Although several reports are available in the literature that deal with EUV radiation–induced growth of contaminants on Ru surfaces,[8] knowledge of the adsorption dynamics and of the emission angle (θ from the target surface) dependency are still scarce. In fact, detailed analyses of the latter will help to figure out which of the components of the adsorbed species are mainly responsible for degrading the mirror performance.

In this communication, we show real time contamination of the Ru surface in the presence of a 13.5-nm wavelength of light using EUV photoelectron spectroscopy (EUPS). This approach is extremely surface sensitive due to low photoelectron escape depth.[9] Using the measured cutoff energy shift, we show the formation of dipoles on the Ru surface. The *in situ* angular-resolved x-ray photoelectron spectroscopy (XPS) has been employed to analyze the chemical behavior of the adsorbents on the Ru surface with varying θ.

All our experiments have been performed at the surface characterization laboratory IMPACT of CMUXE at Purdue University, housing *in situ* facilities like XPS, EUPS, Auger electron spectroscopy, ion scattering spectroscopy, and a setup for EUV reflectivity. More details on the experimental setup can be found elsewhere.[10] Keeping in mind the baking issues to avoid the degradation of the mirror performance,[6] the samples were analyzed in our mildly baked ultrahigh vacuum (UHV) chamber (base pressure $< 1.8 \times 10^{-8}$ Torr) during the experiments. A compact 92 eV source from Phoenix was used to generate 13.5 nm EUV light, while time-dependent EUPS measurements were carried out using a hemispherical analyzer (Specs Phoibos-100), keeping θ at 30° and the azimuthal angle φ at 45° from the electron analyzer. Calibration of the binding energy (BE) scale with respect to the measured kinetic energy (KE) was made using the silver Fermi edge. A 50-nm-thick Ru film grown on a 4-inch *p*-type Si(100) wafer was diced into several pieces with an average area of 1×1 cm^2. Before performing our study, the Ru surface was sputter-cleaned with 2 keV Ar^+, giving a sample current of $\sim$ 800 nA. XPS measurements were performed using an Al-K_α radiation ($h\nu = 1486.65$ eV), and the data were recorded for θ in the range of 0° to 50° with φ at 45°.

Figure 1 exhibits the typical EUPS spectra recoded in 29 consecutive scans, each taking 43 s. As can be seen, the signal in the high KE region is comparatively weaker than the low KE (cutoff) region. Close inspection of the cutoff region reveals that the magnitude of the secondary electron peak intensity is increased with EUV exposure time. This indicates that the Ru surface is gradually covered by the adsorbents[11] until it saturates. This is further confirmed by investigating the change in work function ($\Delta\phi$), which was

[a]Electronic mail: mcatalfa@purdue.edu.

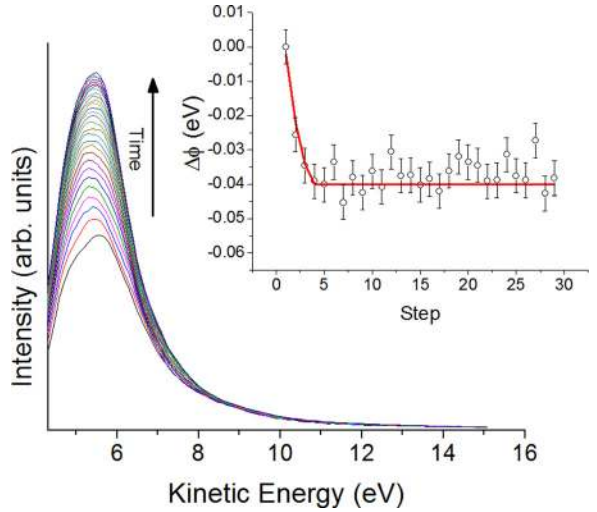

FIG. 1. (Color online) Cutoff region of the EUPS spectra, showing growth of the secondary electrons with EUV exposure time. The change in work function is shown in the inset. Each step lasts for 43 s. The change in orientation of the dipoles is indicated by a solid curve, obtained by fitting the experimental data points (open circles).

derived from the onset of the cutoff region. The inset displays the variation of $\Delta\phi$ with scan step, indicating the formation of dipoles at the adsorbent/Ru interface. It appears (inset) that $\Delta\phi$ saturates after 4 steps, with an initial decrease of –0.04 eV. The negative value indicates that molecules are directed away from the Ru surface. It seems that, after the formation of the first monolayer, there is no more change in orientation of the dipoles at the interface. However, the parallel increase in secondary electrons suggests that the foreign species that are continuously falling onto the first chemisorbed layer are forming physisorbed layers, which do not have any significant impact on the interfacial dipoles.

In order to check the chemical properties of the adsorbents, XPS measurements have been performed, showing the dominance of carbon and water molecules on the Ru surface — in accordance with previous studies.[6] It is now well established that the residual hydrocarbons and water molecules are dissociated during EUV exposure because of the interaction with the secondary electrons.[12] During this process, hydroxyl (OH) radicals are formed due to the dissociation of water molecules, while carbon atoms accumulate onto the Ru surface[3] via splitting of hydrocarbons into smaller and chemically active groups.[7] In fact, the observed time-dependent photoelectron dynamics in the recorded EUPS spectra (Fig. 1) are found to be associated with a competition between the adsorption and/or dissociation of water molecules and hydrocarbons on the Ru surface under EUV exposure, which will be discussed in the following, based on our detailed XPS analyses.

Since the reflectivity and transmission coefficient of the Ru layer depend on incidence angle of the 13.5-nm EUV light, it is now important to know how this light is affected at each angle. According to the geometry of the chamber, when the incidence angle β is 25°, then $\theta = 0°$. Therefore, when θ increases from 0° to 50°, β will change from 25° to –25°. Hence, the coupling between the electric field **E** (which is perpendicular to the beam) and the molecular components will vary with increasing β if they have chemical anisotropy. However, our XPS data show band dispersions in both Ru 3*d* and O 1*s* regions (see Fig. 2). One should not expect such band dispersion, as the core levels are highly localized in nature[13] and should not be affected by the surface contamination. Therefore, any shift seen in the spectrum with θ from 0° to 50° at both the O 1*s* and Ru 3*d* regions (Fig. 2) is due to the variation in coupling between **E** and the components of the adsorbed molecules on the surface.

Both the O 1*s* and Ru 3*d* regions in Fig. 2 show two sets of data: one set is for the Ru surface, which was sputtered at the beginning of the XPS measurements and, thus, was contaminated with time and increasing θ (solid curves), whereas the second set represents the data acquired after sputtering the sample for every θ (dotted curves). Both sets of spectra

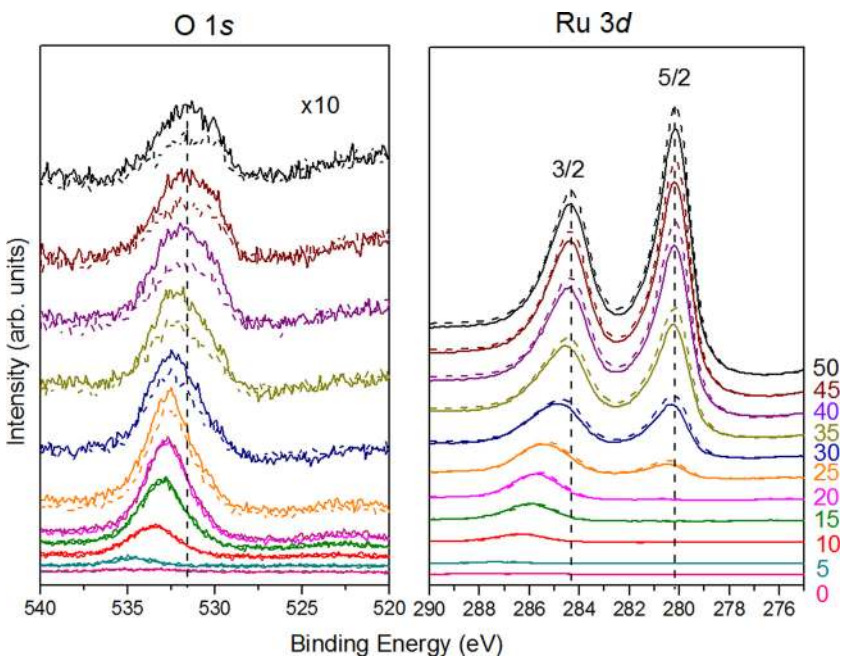

FIG. 2. (Color online) Angle-resolved XPS scans within a range of emission angle from 0° to 50°. Solid lines indicate Ru samples sputtered once in the beginning, while dotted lines indicate continuous sputtering at every angle. Vertical dashed lines are given to guide the eyes to follow the peak dispersion. All O 1*s* curves are multiplied by 10 for clarity.

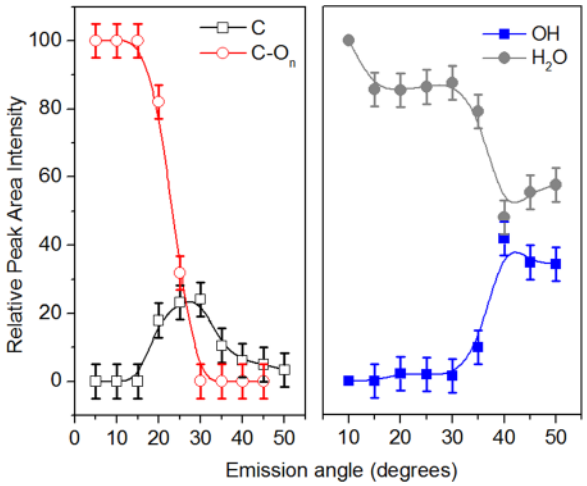

FIG. 3. (Color online) Relative peak area intensity with emission angle in each XPS region. Left panel: C (open squares) and C-O_n (open circles). Right panel: OH (solid squares) and H_2O (solid circles).

indicate that the sputtering effect is almost negligible at lower θ. This is because the water molecules (O 1s region) and C-O_n (Ru 3d region) in the first layer bind directly to the Ru surface and dominate at lower angles (see Fig. 3), due to their orientations. However, the corresponding XPS signals are weak, due to poor photoionization cross-sections in the presence of a limited number of molecules in a single layer. Thus, the Ru 3*d* spin-orbit doublets, such as Ru $3d_{5/2}$ and Ru $3d_{3/2}$, which are peaking around 280.1 and 284.9 eV, respectively, are only prominent for $\theta > 35°$. A clear variation of the peak intensity ratio of the Ru $3d_{5/2}$ and Ru $3d_{3/2}$ is also observed, whereas the O 1*s* peak becomes sharper at lower θ up to 15°. Looking at both O 1*s* and Ru 3*d* regions (Fig. 2), it appears that the change in intensity is pronounced at higher θ, especially in the O 1s region.

For in-depth understanding of the observed facts, XPS spectra recorded at various θ have been deconvoluted into components using a conventional fitting procedure. The components used are the chemically active fragments resulting from the dissociation of hydrocarbons and/or water molecules by secondary electrons[6] created by x-rays. Although we have used Ru and RuO_2 in our fittings, we have considered here only the components associated with the adsorbents on the Ru surface. In particular, we found that water molecules (532.6 eV) and OH radicals (530.75 eV)[14] are the components of interest in the O 1*s* region, whereas the Ru 3*d* region consists of carbon (284.6 eV) and oxidized carbon (i.e., C-O_n), which includes both O–C = O (288.6 eV) and C–O (286.4 eV).[15] The relative change in peak area intensity of water molecules and OH (right panel) and the carbon and C-O_n (left panel) are plotted in Fig. 3. Although β was kept near normal to the Ru surface (25° to –25°), there exists a large change in peak area intensity of the molecular components. This phenomenon can be explained in the light of the variation in coupling between **E** with C-O_n and water molecules at lower θ and hydroxides at higher θ. Interestingly, graphitic carbon shows a parabolic behavior with a peak at 30°. This indicates that most of the carbon atoms are situated on the top position of the underlying Ru atoms, suggesting that the photoionization cross-section decreases on either side of 30° in the presence of varying molecular symmetry. Therefore, we can conclude that the adsorbents are anisotropic in nature on the Ru surface and their components play the decisive role in degrading the EUV reflectivity or optical transmission.

In summary, we have shown time-dependent photoelectron dynamics in the EUPS spectra using 13.5-nm wavelength of light, where the rise of the secondary electrons is explained in terms of the adsorption of contaminants on the Ru surface. In addition, the molecules are proven to form dipoles on the Ru film by measuring the change in work function as a function of EUV exposure time, while the diploes are oriented outward from the surface. Further angle-resolved XPS investigations show the probability of the components of the adsorbed species to couple with the electric field of the incident electromagnetic radiation with increasing θ in the range from 0° to 50°. Such a fast contamination on the Ru surface has also been revealed from angle-resolved XPS measurements. Detailed XPS analyses suggest that the water molecules and C-O_n are the dominant components at lower θ, OH radicals at higher angles; carbon atoms are more probable at the middle regions. Finally, this study reveals which components are responsible at which angle for degrading the reflecting property of the surface Ru layer when the electromagnetic radiation is falling onto the surface in the near normal incidence.

ACKNOWLEDGMENTS

This work is partially supported by SEMATECH and Purdue University.

[1]L. Belau, J. Y. Park, T. Liang, H. Seo, and G. A. Somorjai, J. Vac. Sci. Technol. B **27**(4), 1919 (2009).
[2]H. Over, Y. B. He, A. Farkas, G. Mellau, C. Korte, M. Knapp, M. Chandhok, and M. Fang, J. Vac. Sci. Technol. B **25**(4), 1123 (2007).
[3]B. V. Yakshinskiy, R. Wasielewski, E. Loginova, M. N. Hedhili, and T. E. Madey, Surf. Sci. **602**(20), 3220 (2008).
[4]H. Shin, J. R. Sporre, R. Raju, and D. N. Ruzic, Microelectron. Eng. **86**(1), 99 (2009).
[5]S. Bajt, N. V. Edwards, and T. E. Madey, Surf. Sci. Rep. **63**(2), 73 (2008).
[6]T. E. Madey, N. S. Faradzhev, B. V. Yakshinskiy, and N. V. Edwards, Appl. Surf. Sci. **253**(4), 1691 (2006).
[7]J. Hollenshead and L. Klebanoff, J. Vac. Sci. Technol. B **24**(1), 64 (2006).
[8]J. Chen, E. Louis, C. J. Lee, H. Wormeester, R. Kunze, H. Schmidt, D. Schneider, R. Moors, W. van Schaik, M. Lubomska, and F. Bijkerk, Opt. Express **17**(19), 16969 (2009).
[9]S. Hufner, *Photoelectron Spectroscopy*, 2nd ed. (Springer, Berlin-Heidelberg, 1996).
[10]J. P. Allain, M. Nieto, M. R. Hendricks, P. Plotkin, S. S. Harilal, and A. Hassanein, Rev. Sci. Instrum. **78**(11), 113105 (2007).
[11]R. Schlaf, C. D. Merritt, L. C. Picciolo, and Z. H. Kafafi, J. Appl. Phys. **90**(4), 1903 (2001).
[12]G. Kyriakou, D. J. Davis, R. B. Grant, D. J. Watson, A. Keen, M. S. Tikhov, and R. M. Lambert, J. Phys. Chem. C **111**(12), 4491 (2007).
[13]S. Lizzit, G. Zampieri, L. Petaccia, R. Larciprete, P. Lacovig, E. D. L. Rienks, G. Bihlmayer, A. Baraldi, and P. Hofmann, Nature Phys. **6**(5), 345 (2010).
[14]C. Mun, J. Ehrhardt, J. Lambert, and C. Madic, Appl. Surf. Sci. **253**(18), 7613 (2007).
[15]W. H. Lee, S. J. Kim, W. J. Lee, J. G. Lee, R. C. Haddon, and P. J. Reucroft, Appl. Surf. Sci. **181**(1–2), 121 (2001).